Macromolecules
ARTICLE

Macromolecules **2010**, *43*, 643–651 **643**
DOI: 10.1021/ma902379t

Molecular Dynamics of Natural Rubber/Layered Silicate Nanocomposites As Studied by Dielectric Relaxation Spectroscopy

Marianella Hernández,*,†,‡ Javier Carretero-González,‡ Raquel Verdejo,‡ Tiberio A. Ezquerra,§ and Miguel A. López-Manchado*,‡

†*Universidad Simón Bolívar, Departamento de Mecánica, Valle de Sartenejas, Caracas 1081, Venezuela,* ‡*Instituto de Ciencia y Tecnología de Polímeros, CSIC, Madrid 28006, Spain, and* §*Instituto de Estructura de la Materia, CSIC, Madrid 28006, Spain*

Received October 26, 2009; Revised Manuscript Received December 4, 2009

ABSTRACT: The segmental chain dynamics in nonvulcanized and vulcanized natural rubber/layered silicate nanocomposites has been studied by dielectric relaxation spectroscopy. Special consideration has been devoted to the effect of clay type and loading on the time scale of the relaxation processes. Results reveal that the type and concentration of clay do not have an effect on the segmental mode of the NR matrix, while the vulcanization reaction slows down the segmental dynamics. A new mode, slower than the segmental dynamics but faster than the normal mode associated with the chain dynamics, has been observed for both vulcanized and nonvulcanized nanocomposites with fillers having high levels of intercalation. We attribute the new mode to a restricted segmental dynamics of natural rubber chains located at the clay/rubber interfacial regions.

1. Introduction

Nanotechnology is recognized as one of the most promising fields of research of the 21st century. The beginning of nanotechnology and nanoscience research can be traced back over 40 years. However, it was in the past decade that the world witnessed bigger strides of this technology from both academic and industrial points of view.[1−4]

The term "nanocomposite" refers to every type of composite material having fillers in the nanometer size range, at least in one dimension. For such nanocomposites the total interfacial phase becomes the critical parameter, rather than the volume fraction of the filler.[5−7] Because of their nanofillers dispersion, nanocomposites exhibit markedly improved mechanical, thermal, electrical, and gas barrier properties, when compared to pure polymers or their traditional composites. The most common nanosized fillers are inorganic clay minerals consisting of nanolayered silicates. The stacking of the layers of ∼1 nm thickness by weak dipolar forces leads to interlayers or galleries between the layers. These galleries are occupied by cations such as Na^+ and Ca^{2+} which can be replaced by organic cations such as alkylammonium cations via ion exchange reaction rendering to obtain hydrophobic surfaces. This ion exchange produces organophilic clays called organoclays which are more compatible with the polymer.[8,9] The literature search shows that several research groups have prepared nanocomposites based on plastics and rubbers with nanoclays. In particular, rubber/layered silicate nanocomposites are increasingly attracting scientific and technological attention because of the high reinforcing efficiency of the nanosilicate, even at very low loading (< 10 wt %).[10−13] Without the filler, rubber formulations would yield resilient products having elastic properties but very little strength. So, strength properties are introduced by the addition of rigid entities such as nanosilicates, and the inclusion of these nanofillers to rubber formulations results in optimization of properties, especially to meet given application or sets of performance parameters. The high specific surface area is believed to be one of the reasons why the nature of reinforcement is different in composites based on nanofillers. It is expected to provide enhanced interphase effects and tensile strength. Nevertheless, there is yet no satisfactory theoretical explanation for the origin of improvement of the properties of polymer nanocomposites.[14,15] Results obtained by various experimental techniques, as well as by theory and computer simulations, indicate the presence of an interfacial polymer layer around the filler, with structure/morphology and chain dynamics modified with respect to the bulk polymer matrix.[7,15−17]

Broadband dielectric spectroscopy is a powerful tool for the investigation of molecular dynamics of polymers and composites. Dielectric property analysis of filled polymers contributes to a better understanding of the structure−property relationships at the morphological level. More specifically, in order to relate the macroscopic properties of nanocomposites with molecular concepts, one must understand the molecular motions or dynamics of these materials in response to various applied fields.

When placed in an electric field, nanocomposites are subjected to ionic, interfacial, and dipole polarization. These polarization mechanisms have considerable different time and length scales, making dielectric spectroscopy uniquely suited for the study of nanocomposite dynamics.[18] Therefore, motional processes which take place for polymeric systems on extremely different time scales can be investigated in a broad frequency and temperature range. Such motional processes can be localized fluctuations within a backbone segment or local rotational fluctuations of a short side chain. On a larger spatial and longer time scale and for temperatures above the glass transition the so-called segmental motion or α-relaxation becomes relevant. At more extended length scale, for polymers with a component of the dipole moment parallel to the chain, a further process can be observed called normal-mode relaxation, in which the translational motion of the whole chain characterized by the end-to-end vector takes place. In this case, the molecular dipole vectors that are parallel to

*Corresponding authors. E-mail: marherna@ictp.csic.es or marherna@usb.ve (M.H.); lmanchado@ictp.csic.es (M.A.L.-M.).

Published on Web 12/11/2009

Table 1. Technical Characteristics of the Layered Silicates Employed in This Work

clay	organic modifier	modifier concn (mequiv/100 g clay)	basal spacing, d (nm)
Cloisite Na^+ (CNa+)	none		1.1
Cloisite 15A (C15A)	2M2HT[a]	125	~3.0

[a] 2M2HT: dimethyl, dehydrogenated tallow, quaternary ammonium. The tallow consists of ~65% of C_{18}, ~30% of C_{16}, and ~5% of C_{14} and a chloride anion.[26]

the repeating unit are summed up over the chain, and therefore the normal-mode relaxation is related to both the shape and the dynamics of the macromolecule.[19−21]

Several authors have extensively studied the dynamics of 1,4-*cis*-poly(isoprene) (PI) by using dielectric spectroscopy.[18,22−25] Because of the lack of symmetry in its chemical structure, PI has nonzero components of the dipole moment both perpendicular and parallel to the chain contour. Thus, two dielectric relaxation processes, the segmental- and the normal-mode process, are present. Moreover, Mijovic et al.[18] have studied nanocomposites of organically modified clay nanoparticles and a nonvulcanized PI matrix prepared by solution-mediated intercalation. A direct comparison of dielectric relaxation spectroscopy and dynamic mechanical spectroscopy results, made by deconvolution of dielectric and viscoelastic spectra, showed excellent agreement between the average relaxation time for both segmental and normal mode relaxation.Nonetheless, to our best knowledge no in-depth study of the dielectric properties of natural rubber (NR) nanocomposites has been undertaken, analyzing the relaxation spectra and correlating the molecular motion of chains with its structure.

Therefore, the aim of this paper is to study the effect of the presence of the filler on the local and global motions of polymer chains in NR/nanolayered silicate composites. At first, we report results from dielectric spectroscopy, examining how the segmental and normal modes of these polymer chains are affected by the presence of silicate particles. In addition, we show the effect of the concentration of clay on the time and length scale of the relaxation processes, plus a comparison between nanosilicates. We also discuss on the influence of the vulcanization and how the cross-linking process affects the dielectric spectra of the nanocomposites.

2. Experimental Section

2.1. Materials. Natural rubber (NR) was kindly supplied by Malaysian Rubber (Berhad, Malaysia) under the trade name CV 60 (Mooney viscosity: ML(1 + 4) 100 °C = 60). Two layered silicates were employed in this study, in particular, a natural sodium montmorillonite described as Cloisite Na^+ (CNa+) and this montmorillonite modified with a quaternary ammonium salt, Cloisite 15A (C15A). Both samples were provided by Southern Clay Products Inc. (Gonzales, TX). The structural characteristics of the clays are reported in Table 1.

2.2. Preparation of NR Nanocomposites. Nonvulcanized nanocomposites were prepared consisting of the pure gum and the layered silicate (1, 2.5, 5, 7.5, and 10 phr (parts per hundred of rubber)). The samples are referred to as NR/xy, where x and y correspond to the amount and type of clay, respectively. With respect to the vulcanized samples, the formulation of natural rubber compounds expressed as (phr) is as follows: sulfur (2.5), zinc oxide (5), stearic acid (1), MBTS (benzothyazyl disulfide) (1), antioxidant PBN (phenyl-β-naphthylamine) (1), and layered silicate (5 and 10). The nanocomposite samples were prepared in an open two-roll laboratory mill at room temperature. The rotors operated at a speed ratio of 1:1.4. Rubber compounds were vulcanized at 150 °C in an electrically heated hydraulic press using the optimum cure time (t_{90}) derived from the curing curves previously determined by means of a rubber process analyzer (RPA2000 Alpha Technologies). These samples are referred to as vulcNR/xy, following the same nomenclature as for the nonvulcanizates. Identical methodology was applied to both layered silicates nanocomposites (NR/C15A and NR/CNa+), thus affording a quantitative comparison of their dynamics.

2.3. Characterization. Broadband dielectric relaxation spectroscopy (DRS) measurements were performed on an ALPHA high-resolution dielectric analyzer (Novocontrol Technologies GmbH, Hundsangen, Germany). Film samples prepared from the nanocomposites were mounted in the dielectric cell between two parallel gold-plated electrodes. The complex permittivity ε^* of a given sample can be calculated from the measurement of the complex impedance Z^* given by

$$Z^*(\omega) = \frac{U^*(\omega)}{I^*(\omega)} \tag{1}$$

where U^* and I^* are the voltage and current circulating through the sample at a certain angular frequency ω. Once the impedance has been measured, ε^* can be calculated by means of

$$\varepsilon^*(\omega) = \varepsilon' - i\varepsilon'' = \frac{1}{i\omega Z^*(\omega) C_0} \tag{2}$$

where ε' and ε'' are the real and imaginary part of the complex permittivity and C_0 corresponds to the capacity of the empty sample holder. The complex permittivity of the nanocomposites was measured over a frequency window of $10^{-1} < F/\mathrm{Hz} < 10^7$ ($F = \omega/2\pi$ is the frequency of the applied electric field) in the temperature range from −150 to 150 °C in 5 °C steps.

The imaginary part of the obtained dielectric permittivity was analyzed by the phenomenological Havriliak−Negami (HN) function[19,27]

$$\varepsilon^*(\omega) = \varepsilon_\infty + \frac{\Delta\varepsilon}{[1 + (i\omega\tau_{\mathrm{HN}})^b]^c} \tag{3}$$

where $\Delta\varepsilon = \varepsilon_S - \varepsilon_\infty$; ε_∞ and ε_S are the unrelaxed and relaxed values of the dielectric constant and τ_{HN} is a characteristic relaxation time. In eq 3, b and c are shape parameters ($0 < b$, $c \leq 1$) which describe the symmetric and the asymmetric broadening of the equivalent relaxation time distribution function, respectively.

Differential scanning calorimetry (DSC) measurements (Perkin-Elmer DSC7) in the temperature range from −75 to 75 °C were also employed to investigate thermal transitions.

3. Results and Discussion

3.1. Broadband Dielectric Relaxation Spectroscopy (DRS) of NR Nanocomposites. Figure 1 describes the dielectric loss spectra for neat NR and its nanocomposites over a wide range of frequency at different temperatures. In all the spectra, the loss peaks are shifting to higher frequencies with increasing temperature. This shift in the frequency of the maxima is characteristic of thermal activated processes.

Similarly to synthetic 1,4-*cis*-poly(isoprene) (PI),[18,22,23,25] two relaxation modes are present in the NR (Figure 1a). For temperatures above the glass transition temperature (T_g = −64 °C) the segmental mode related to the segmental motions of the polymer chain is observed. At higher temperatures, a more intense process which can be assigned to the normal mode is clearly detected. In both nanocomposites (Figure 1b,c) the segmental mode, or α-relaxation, is still detectable and appears located in the same temperature range as for neat NR. A second process appears at higher temperatures in the NR/5C15A composite (Figure 1b) which apparently differs from the normal mode of neat NR.

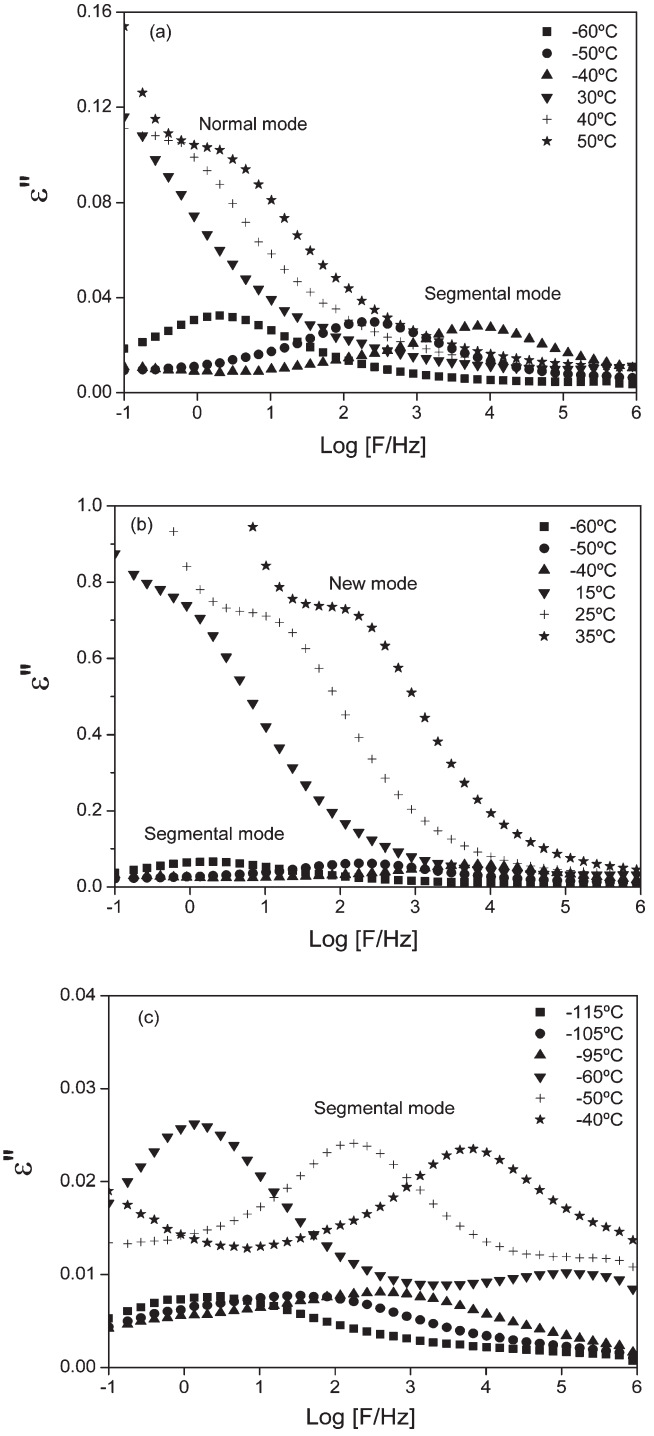

Figure 1. Dielectric loss ε'' vs frequency for (a) neat NR, (b) NR/5C15A nanocomposite, and (c) NR/5CNa+ nanocomposite.

We will refer to this process hereafter as the "new mode" which will be further discussed. This new mode seems to be absent in the NR/5CNa+ nanocomposite (Figure 1c) which only exhibits the segmental mode and an additional process at low temperatures most likely due to the electric dipole rotations of the absorbed water in the silicate gallery.[14,28] Moreover, at high temperatures conductivity dominates the low-frequency tail of the spectrum of the NR/5CNa+ composite; thus, no defined relaxation process can be appreciated.

In order to better examine the different relaxations present in all compounds, the discussion of our results will be divided into low- and high-temperature processes.

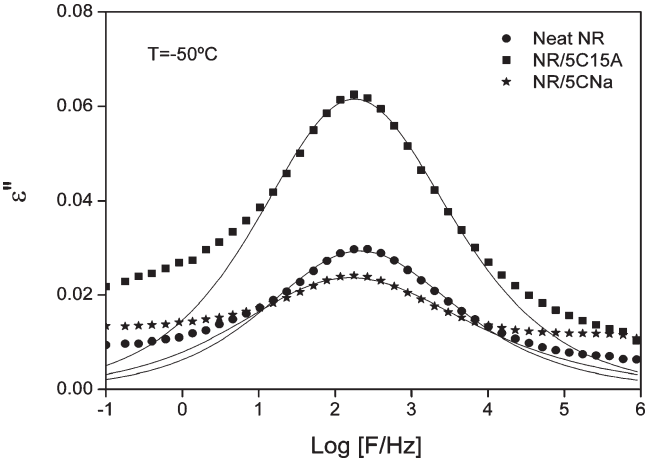

Figure 2. Frequency dependence of dielectric loss ε'' of the NR nanocomposites indicated on the plot in the region of the segmental mode. Solid lines correspond to HN fitting.

Table 2. HN Parameters of Segmental Mode of NR and Its Nanocomposites

compound	T (°C)	$\Delta\varepsilon$	b	c	τ_{HN} (s)
neat NR	−55	0.150	0.492	1	6.093×10^{-3}
	−50	0.145	0.493	0.987	7.557×10^{-4}
	−45	0.140	0.557	0.683	2.383×10^{-4}
NR/5C15A	−55	0.314	0.522	0.832	1.031×10^{-2}
	−50	0.308	0.497	0.924	1.032×10^{-3}
	−45	0.292	0.505	0.938	1.537×10^{-4}
NR/5CNa+	−55	0.140	0.439	0.937	1.001×10^{-2}
	−50	0.143	0.448	0.749	1.863×10^{-3}
	−45	0.142	0.433	0.811	2.261×10^{-4}

3.1.1. Low-Temperature Process: Segmental Relaxation. Figure 2 shows selected dielectric loss spectra at $T = -50$ °C for NR and the NR/5C15A and NR/5CNa+ nanocomposites. From the spectra hereby presented, we can notice that the segmental mode process (α-relaxation) is well resolved in the frequency domain and shows a relatively broad and asymmetric peak regardless the type of filler incorporated in the nanocomposite if compared to the spectrum of neat NR. These results suggest the independence of the glass transition process with the silicate incorporated. Besides, the invariance of the glass transition has been verified when the silicate type content varies from 1 to 10 phr. Thus, no significant changes on the segmental molecular dynamics of the NR come into sight by the addition of layered nanosilicates in the bulk state.

One can also see that all three spectra can be well described by the HN function. The characteristic parameters of this function (see eq 3) such as $\Delta\varepsilon$, b, c, and τ_{HN} were obtained. Table 2 shows these parameters for temperatures in the region of the segmental mode.

We corroborated that the position of the segmental mode was independent of silicate type and content by analyzing the temperature dependence of the relaxation time (τ_{max}) obtained from the HN fitting parameters

$$\tau_{max} = \frac{1}{2\pi F_{max}} = \tau_{HN}\left[\sin\frac{b\pi}{2+2c}\right]^{-1/b}\left[\sin\frac{bc\pi}{2+2c}\right]^{1/b} \quad (4)$$

The corresponding values for τ_{max}, shown in Figure 3, reveal the Vogel−Fulcher−Tamman (VFT) dependence of τ_{max} with the reciprocal temperature as

$$\tau_{max} = \tau_0 \exp\left(\frac{B}{T - T_0}\right) \quad (5)$$

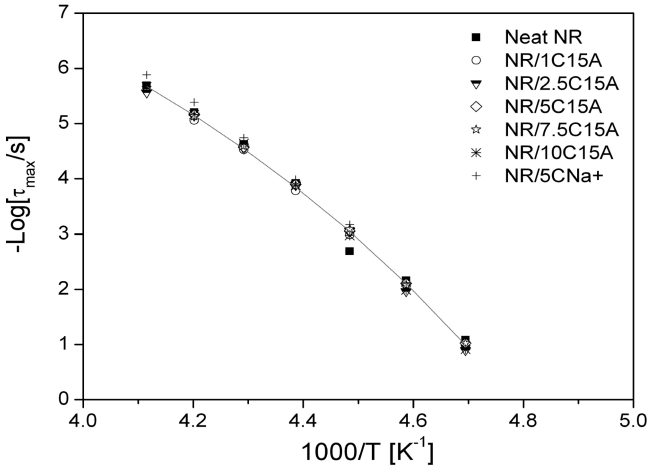

Figure 3. Temperature dependence of the average relaxation time for the segmental mode of NR and its nanocomposites with clay loading as a parameter.

where τ_0 and B are empirical parameters, and T_0 is the so-called ideal glass transition or Vogel temperature, which is generally 30−70 K below T_g.[20] To reduce the effect of data fitting to the VFT equation over a limited frequency range, a value of log $\tau_0 \approx 14$ s was assumed according to previous work.[29]

In Figure 3 we can clearly see that neither an increase in nanosilicate loading nor the type of filler added has an effect on the time scale of the segmental mode process of the NR matrix.

3.1.2. High-Temperature Processes: New and Normal Modes. Figure 4a shows selected dielectric loss spectra at $T = 40$ °C for NR and the NR/5C15A and NR/5CNa+ nanocomposites in the temperature region where the "new mode" is observed for the NR/5C15A. From the spectra presented in this figure, we observe that neither NR nor NR/5CNa+ exhibit this new mode, being only detectable for the nanocomposite with the additive C15A. The nanoclay C15A is a montmorillonite modified with a quaternary ammonium salt. This modification results in a more pronounced intercalation of the NR chains, as corroborated by previous studies.[11,12,14] According to the X-ray diffraction (XRD) spectra presented in Figure 5, it is clear that a pronounced intercalation is achieved by the incorporation of the C15A clay. In fact, the high-intensity characteristic peaks at $2\theta = 3.2°$ and $2\theta = 7.1°$ of the C15A disappear, providing a strong evidence of the insertion of the elastomer into the silicate galleries, disrupting the regular stacked-layer structure of the organoclay and giving rise to an exfoliated structure. In the case of the CNa+ nanocomposite, the characteristic peak at $2\theta = 7.8°$ also disappears. Nonetheless, this result might be a consequence of the low intensity of the diffraction peak of the CNa+ and low content of clay present in the composite and not to the intercalation of NR chains. Transmission electron microscopy (TEM) images presented in Figure 5 confirm that the C15A silicate layers are better exfoliated and randomly dispersed throughout the elastomer matrix as monolayers, while the incorporation of the unmodified clay CNa+ only gives rise to a conventional composite at a microscopic scale.

Therefore, we could expect a restricted mobility of the polymer chains close to the polymer/filler interface due to an enhanced interaction of the NR chains with the clay surface. These interactions should not be present in the unfilled NR matrix or conventional NR composites with poorer intercalation as in those based on unmodified clay (CNa+).

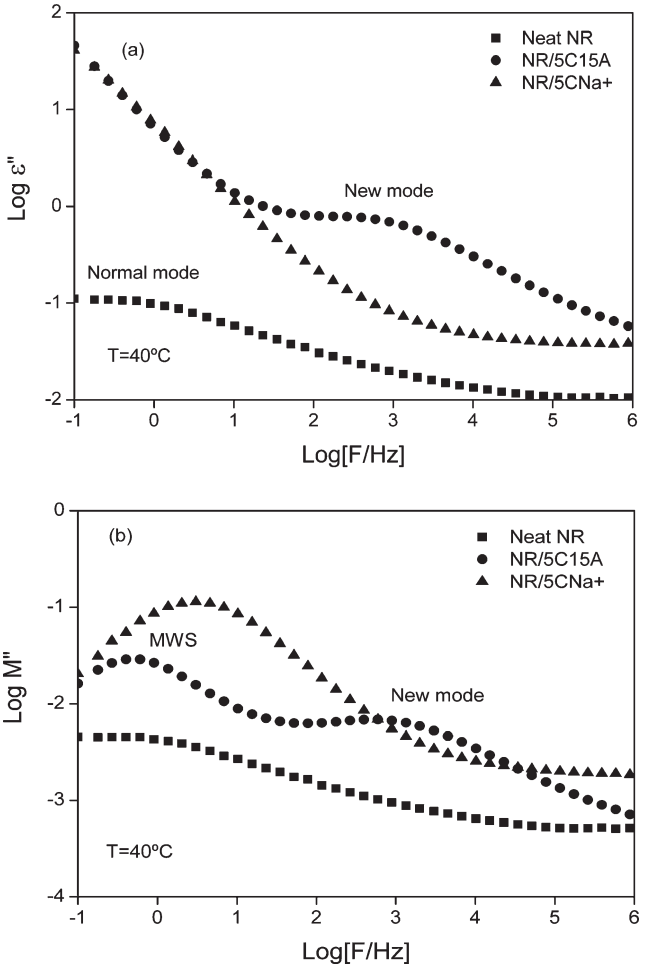

Figure 4. (a) Dielectric loss ε'' and (b) dielectric loss modulus M'' in the frequency domain for neat NR and its nanocomposites.

In order to better understand the physical nature of the new mode, the dielectric modulus formalism was employed (see Figure 4b). The permittivity and modulus formalisms describe the same electrical relaxation phenomena; however, under different conditions a specific formalism could allow to extract more information with respect to the occurring physical processes. In this study, the recorded dielectric data were initially expressed in terms of real and imaginary part of permittivity and then transformed, via eq 6, to the electric modulus formalism:

$$M^* = \frac{1}{\varepsilon^*} = \frac{1}{\varepsilon' - i\varepsilon''} = \frac{\varepsilon'}{\varepsilon'^2 + \varepsilon''^2} + i\frac{\varepsilon''}{\varepsilon'^2 + \varepsilon''^2}$$
$$= M' + iM'' \quad (6)$$

where M' is the real and M'' the imaginary part of the electric modulus. In particular, the interpretation of relaxation phenomena via the electric modulus formalism offers some advantages upon other treatments, since large variations in the permittivity and loss at low frequencies and high temperatures are minimized. Further, difficulties occurring from the electrode nature, the electrode−specimen contact, and the injection of space charges and absorbed impurities can be neglected. Arguments and examples for the resulting benefits of the electric modulus presentation have been presented elsewhere.[30,31]

The modulus spectra of nanocomposites offer an added insight into their dynamics because high conductivity makes

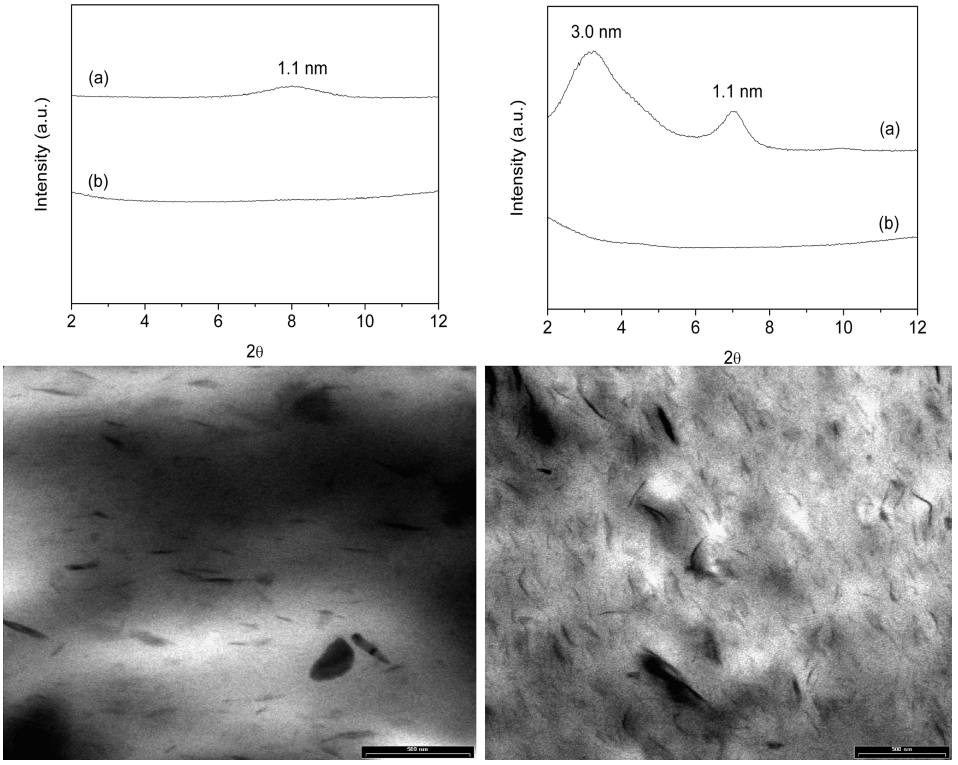

Figure 5. Top left: XRD patterns of (a) CNa+ and (b) NR/5CNa+. Top right: XRD patterns of (a) C15A and (b) NR/5C15A. Bottom left: TEM image of NR/5CNa+ nanocomposite. Bottom right: TEM image of NR/5C15A nanocomposite. The scale bar corresponds to 500 nm.

identification of relaxation processes in the permittivity spectra difficult, though not impossible.[32] Figure 4b shows the dielectric modulus spectra of the pure gum, NR, and its nanocomposites (NR/5C15A and NR/5CNa+). In the low-frequency region, a relaxation process can be observed in the nanocomposites regardless of the type of clay added, while this process is absent in the pure NR. The incorporation of nanoclay caused additional relaxation dispersion due to an interfacial polarization at the nanoclay/polymer interface, the so-called Maxwell−Wagner−Sillars (MWS) effect. The MWS relaxation refers to the frequency dependence of interfacial polarization (ion accumulation) that occurs at the interface between materials with differing dielectric constants, such as polymer and layered silicate. The MWS transition is expected at the low-frequency range and involves rather high ε' and ε'' values.[33] Interfacial polarization is always present in materials comprised of more than one phase. This kind of polarization arising at the interfaces is due to the migration of charge carriers through different phases of the composite material resulting in differential charge accumulation at the interfaces. When these charges are made to move by the application of an external electric field, the motion will be hindered at various points of the composite material differently, causing space charge to appear. The appearance of such space charge can distort the macroscopic field and appears as polarization to an external observer.[34]

Figure 4b also reveals for the NR/5C15A nanocomposite the presence of the "new mode" reflected in Figure 4a accompanied at lower frequencies by the MWS interfacial polarization.

Some interesting features can be noted regarding the influence of clay content on the "new mode" by representing the dielectric strength of the "new mode" as a function of the filler content (Figure 6) for the NR/C15A nanocomposites. Here we can notice a slight increasing tendency in dielectric

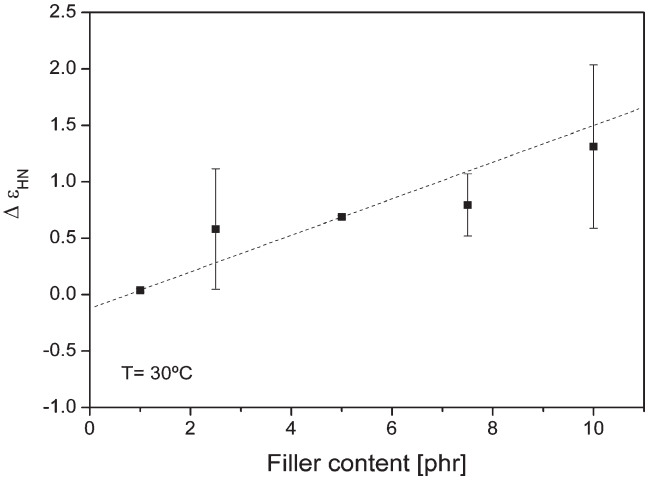

Figure 6. Relaxation strength as a function of clay loading for the NR/C15A nanocomposites.

strength ($\Delta\varepsilon$) with clay loading. This behavior could induce us to assign the "new mode" to a phase of the polymer close to the polymer/filler interface.

The average relaxation times of the "new mode" observed for the NR/C15A nanocomposites have been represented in Figure 7 as a function of the reciprocal temperature for different filler contents. The data presented in Figure 7 reveal that this new relaxation becomes faster with increasing filler content. In order to illustrate this effect, Figure 8 shows the temperatures at which the average relaxation time of the new mode reaches a value of 0.1 s. It becomes evident the "new mode" speeds up with filler content and levels off for loadings higher than 5 phr. In principle, one would expect confinement effects to be increasingly important as filler content increases. In general, segmental dynamics may

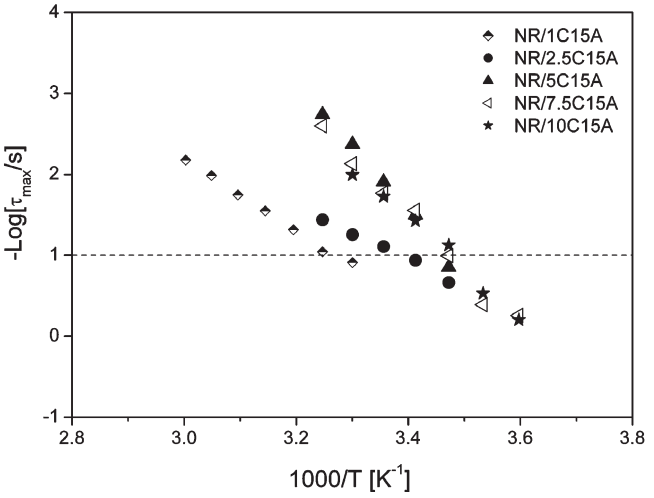

Figure 7. Temperature dependence of the average relaxation time for the "new mode" of NR/C15A nanocomposites with clay loading as a parameter.

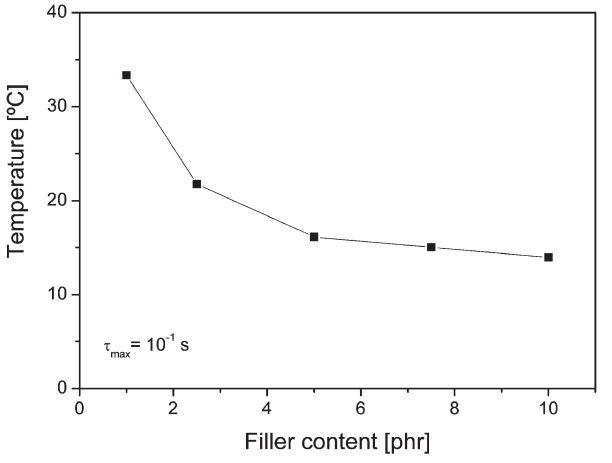

Figure 8. Temperature dependence of the "new mode" at $\tau_{max} = 10^{-1}$ s for NR/C15A nanocomposites with clay loading.

become faster by confinement when the confinement volume becomes comparable to that of the cooperative rearranging regions.[35]

In our case, the fastening of the "new mode" dynamics with increasing filler content can be understood as due to a reduction of volume available for the polymer chains intercalated within the galleries formed by the silicate layers. This would imply that an increasing number of layered silicates accommodate NR chains in the central area of the intergallery without expanding the basal spacing, thus resulting in increased relaxation rate.[18,30,36] Interestingly, however, when higher content of clay is added (up to 10 phr), one could presume that a percolated network of nanoparticles that can influence relaxation could be formed, resulting in additional restriction effects. Nevertheless, this issue awaits more detailed and systematic study.

In order to further characterize the "new mode" present in the NR/C15A nanocomposites, DSC measurements were performed. Figure 9 shows DSC heating thermograms of neat NR and four nanocomposites with the clay content (in phr) indicated on the plot. A single glass transition around −70 °C is observed for all samples. This evidence that the thermodynamic glass transition of NR/C15A nanocomposites corresponds to the NR matrix, in agreement with the dielectric data shown in Figure 2 for the segmental mode.

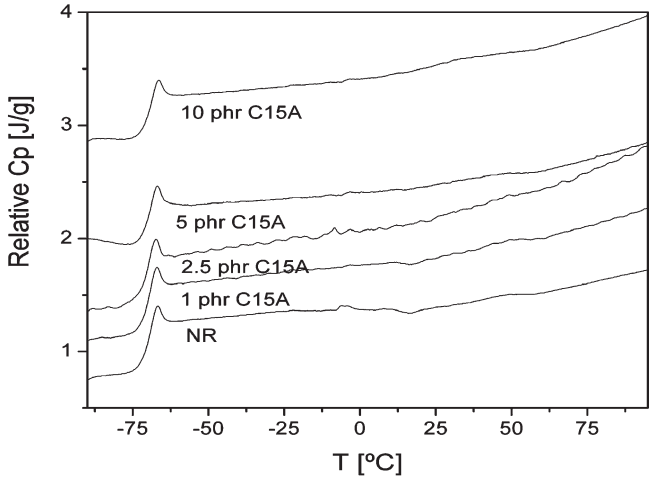

Figure 9. DSC heating thermograms (second runs, displaced vertically for clarity) obtained for NR and the NR/C15A nanocomposites with the clay content indicated on the plot.

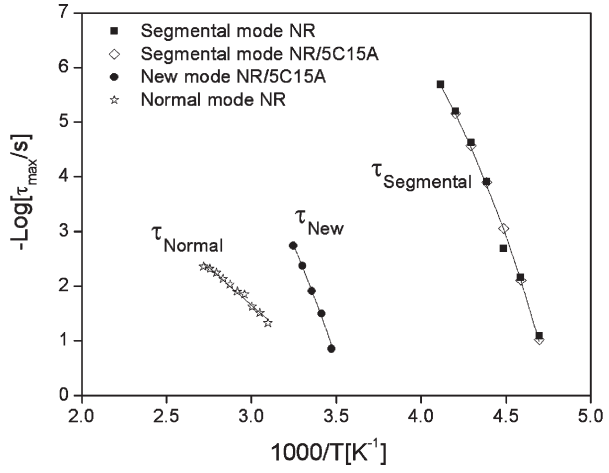

Figure 10. Temperature dependence of the average relaxation time for normal, new, and segmental mode of neat NR and its nanocomposites. Solid lines are fits to the VFT functional form.

At first glance, there is no evidence of a second thermodynamic T_g which could be directly related to the "new mode". However, it has been recently demonstrated using computer simulations that a continuous distribution of relaxation times as we approach a solid interface can lead to a double loss peak in the susceptibility, and this has been proposed as an alternative interpretation for this kind of response.[16,37,38]

Normal mode was examined next. If we analyze the spectrum of neat NR (Figure 1a), we can clearly see that the normal mode process is present at high temperatures at frequencies below the α-process and overlapped with the electrical conductivity contribution. The overall chain dynamics is reflected by this process.

A careful analysis of the VFT temperature dependence of the high-temperature processes (Figure 10) evidence that the global chain dynamics (normal mode) of NR is slower than the segmental mode and exhibits weaker temperature dependence than that of the α-relaxation. This can be understood by considering that the segmental motion proves smaller length scales than those proven by the normal mode process.[19] In between the normal and the segmental modes of the NR matrix, lays the "new mode" of the NR/C15A nanocomposites. For the sake of clarity in Figure 10 only data for the NR/5C15A nanocomposite have been shown. The "new

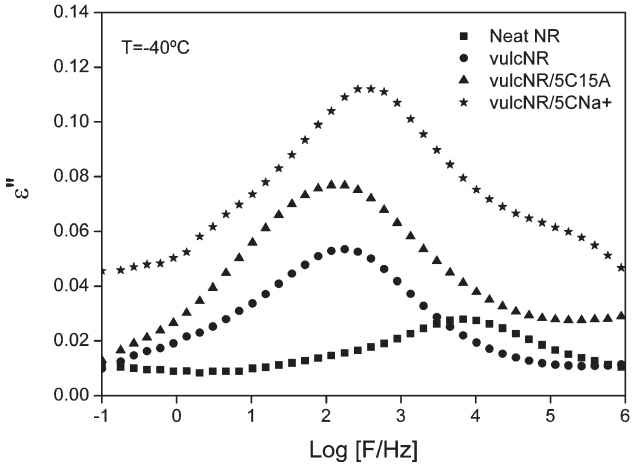

Figure 11. Frequency dependence of dielectric loss ε'' for vulcanized samples of NR and NR/5C15A and NR/5CNa+ nanocomposites in the temperature region of the segmental dynamics. The corresponding spectrum for neat NR is also shown.

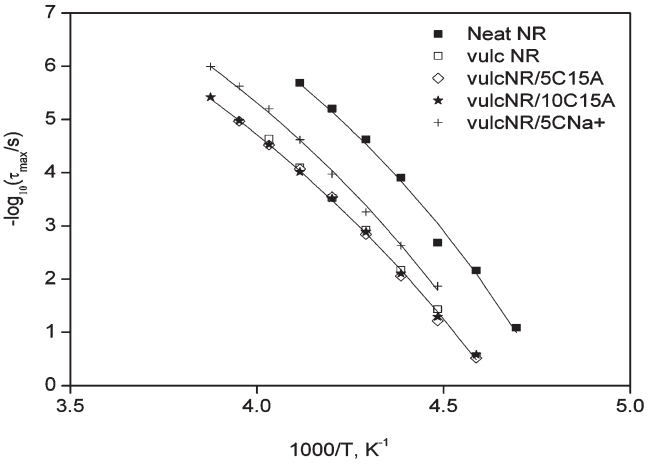

Figure 12. Temperature dependence of the average relaxation time of the segmental mode corresponding to vulcanized samples of NR and NR/C15A and NR/CNa+ nanocomposites.

mode" is clearly slower than the segmental mode but faster than the normal mode process of NR.

Petychakis et al.[39] have investigated the effect of confinement on the global chain dynamics of polyisoprene in controlled porous glass media. They found that for high molecular weights (7K and 10K) the normal mode speeds up due to the effective shorter chains which flow out from the pores. In a similar way, Serghei et al.[40] studied the dynamics in thin films of *cis*-1,4-polyisoprene. They found that if the thickness of the polymer layer becomes comparable to the radius of gyration of the chain, a confinement-induced mode is detected being assigned to fluctuations of terminal subchains, which develop due to immobilization of polymer segments in interaction with a confining interface. This confinement-induced mode becomes faster with decreasing film thickness. These two interpretations could lead us to think that the "new mode" present in the NR/C15A nanocomposite could be a faster normal mode. Nonetheless, in order to complement the analysis about the nature of the "new mode" observed in the NR/C15A nanocomposites and to confirm whether or not the above interpretations are a possible explanation to our findings, we will evaluate the vulcanized NR/silicate nanocomposites.

3.2. Vulcanized NR Nanocomposites. The dielectric measurements have been proven to be useful for studying vulcanization of various kinds of rubber. The most common method of vulcanizing rubber is to mix it with sulfur and heat it up to 100−150 °C. This procedure results in cross-linking of the polymer chains by mono- or polysulfide bridges. A side reaction is also known to proceed along cross-linking, leading to formation of heterocyclic groups in the polymer chains. In sulfur vulcanizates correspondingly the following polar groups are found: (a) the carbonyl groups present in the unvulcanized rubber and those formed during vulcanization; (b) mono- or polysulfide cross-links; (c) S−C bonds in the heterocyclic groups in the main chains.[33] In particular, in vulcanized NR, the change in the segmental mobility is generally observed as a shift of the glass−rubber transition to higher temperatures and an increase in the dispersion amplitudes.[33] Additionally, the normal mode vanishes due to the cross-linking.

In the following sections, the relaxation phenomena present in sulfur vulcanized NR and in vulcanized NR/layered silicate nanocomposites are discussed.

3.2.1. Effect of Vulcanization on the Segmental Dynamics. For the sake of comparison, Figure 11 shows the dielectric loss data for the vulcanized samples of NR, NR/5C15A, and NR/5CNa+ in the temperature region of the segmental dynamics. The corresponding spectrum for nonvulcanized NR is also shown. The results indicate that vulcanizing by sulfur induces a slowing down of the segmental dynamics and a significant increase of the dispersion amplitudes. The later effect indicates that the side reaction resulting in heterocyclic groups is effective because they would hinder the segmental motion, and they would increase the total number of polar groups involved, with a subsequent increase of the dispersion amplitude or the loss maximum.[33]

Figure 12 shows the relaxation times of the segmental mode corresponding to vulcanized samples of NR, NR/5C15A, NR/10C15A, and NR/5CNa+. The relaxation times for nonvulcanized NR have been also included. The observed increase in the average relaxation time due to the vulcanization reaction can be interpreted straightforward considering the network formation. It is evident that the formation of polysulfide cross-links and cyclic sulfide structures cause restrictions on the segmental motions of the polymer chains. Moreover, this high-frequency process exhibits almost no dependence on the degree of filling (5 and 10 phr of C15A). With respect to the relaxation time for the vulcanized NR/5CNa+ nanocomposite, a further detailed comparative study will be reported in the future.

3.2.2. Effect of Vulcanization on the New and Normal Mode Dynamics. For the sake of comparison, Figure 13a shows the dielectric loss data for the vulcanized samples of NR, NR/5C15A, and NR/5CNa+. The selection of the spectra at T = 90 °C was made with the intention of studying the temperature region where the normal mode of unvulcanized NR and the "new mode" of unvulcanized NR/5C15A were previously detected. It is clear the absence of a normal mode in the vulcanized samples. It is known that the normal mode of vulcanized NR becomes broader and decreases in amplitude upon vulcanization due to suppression of large-scale motions of the dipole oriented parallel to the polymer backbone.[19] However, the process corresponding to the "new mode" is present for the vulcanized NR/5C15A nanocomposite. Once again, we used the modulus formalism to better analyze this relaxation.

Figure 13b illustrates the dielectric modulus spectra of vulcanized NR and its nanocomposites. The peak at low frequencies corresponds to the MWS relaxation. In particular,

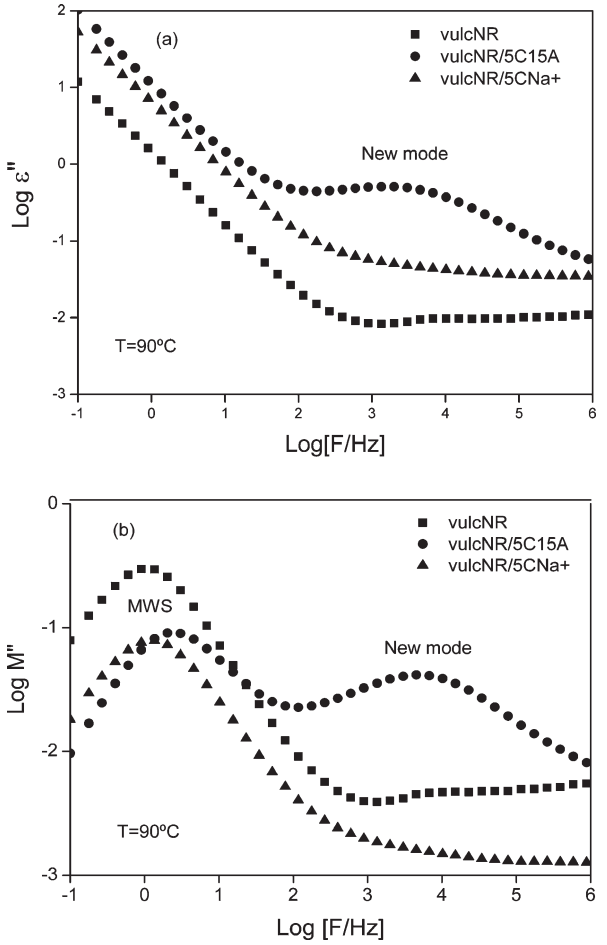

Figure 13. (a) Dielectric loss ε'' and (b) dielectric loss modulus M'' in the frequency domain for vulcanized samples of NR and NR/5C15A and NR/5CNa+ nanocomposites.

in the vulcanized NR compound, this peak can be a consequence of the ingredients (sulfur, accelerators, activation complex, etc.) added to the rubber matrix so the cross-linking reaction can take place. The addition of these components makes the polymeric material to be a heterogeneous media consisting of different phases with different dielectric permittivities and conductivities.[41−43] While for the vulcanized nanocomposites, the presence of the MWS peak has the same explanation as for the nonvulcanized nanocomposites: the interfacial polarization (ion accumulation) that occurs at the interface between materials with differing dielectric constants, such as rubber and layered silicates.

At high frequencies the spectrum of the vulcanized NR/5C15A nanocomposite has similarities with that of the nonvulcanized NR/5C15A nanocomposite, since we note the presence of a second peak associated with the "new mode".

The relaxation times of the segmental mode and "new process" for the vulcanized samples are shown in Figure 14 as a function of the reciprocal temperature. One can clearly see that the "new mode" is also slower than the segmental one for the vulcanized samples. Similarly as previously discussed for the nonvulcanized samples, this effect can be understood by assigning the "new mode" as being caused by a restricted segmental dynamics. Accordingly, the "new mode" can be associated with cooperative movements of polymer chains in the interface layer around the clay particles. The "new mode" is present independently of whether or not the rubber matrix has been vulcanized. We can notice

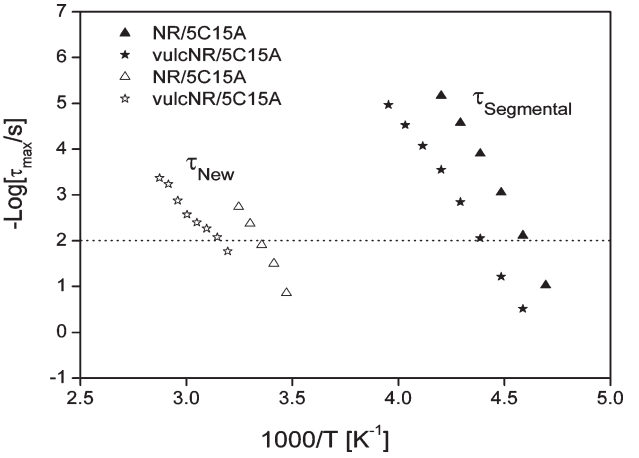

Figure 14. Temperature dependence of the average relaxation time for the segmental and "new" modes of nonvulcanized and vulcanized samples of NR/5C15A nanocomposites.

that both segmental and new mode exhibit equivalent shifts in temperature with vulcanization. Thus, this fact further supports the assumption drawn from the nonvulcanized nanocomposites study suggesting that the "new mode" present in the NR/C15A compounds corresponds effectively to a restricted segmental relaxation. We believe that part of the polymer chains are partially immobilized as an interface layer around the clay particles, and so the interfacial effects dominate the bulk properties of the material.

4. Conclusions

1. Dielectric relaxation spectroscopy has been proven to be a powerful technique for investigating molecular dynamics in a series of nanocomposites consisting of NR and C15A and CNa+ layered silicates.

2. Dielectric measurements show that neither an increase in nanosilicate loading nor the type of filler added has an effect on the segmental mode process of the nonvulcanized NR matrix.

3. The Maxwell−Wagner−Sillars effect is present in all nanocomposites and is attributable to the interfacial polarization at the nanoclay/polymer interface.

4. A new mode ascribed to a restricted segmental mode appears in the NR/C15A nanocomposites regardless of the vulcanization of the NR matrix. This "new mode" has been attributed to the segmental dynamics of polymer chains at the interfacial polymer−particle regions.

5. The absence of the "new mode" for the NR/CNa+ nanocomposites suggests that the appearance of this mode will be associated with silicate fillers with high degree of intercalation.

Acknowledgment. The authors thank the financial support of the Spanish Ministry of Science and Innovation (MiCINN) through the projects MAT2007-61116 and MAT2009-07789. M. Hernández gratefully acknowledges the Misión Ciencia fellowship from the Venezuelan Ministry of Science and Technology and Dr. Alejandro Sanz for his help with the DSC measurements. Dr. R. Verdejo acknowledges a Ramón y Cajal Contract from MiCINN.

References and Notes

(1) Winey, K. I.; Vaia, R. A. *MRS Bull.* **2007**, *32* (4), 314–319.
(2) Okada, A.; Usuki, A. *Macromol. Mater. Eng.* **2006**, *291* (12), 1449–1476.
(3) LeBaron, P. C.; Wang, Z.; Pinnavaia, T. J. *Appl. Clay Sci.* **1999**, *15* (1−2), 11–29.
(4) Giannelis, E. P. *Appl. Organomet. Chem.* **1998**, *12* (10−11), 675–680.

(5) Vaia, R. A.; Wagner, H. D. *Mater. Today* **2004**, *6*, 32–37.
(6) Ray, S.; Easteal, A. J. In *Advances in Polymer-Filler Composites: Macro to Nano*; International Composites Conference, Sydney, Australia, July 11−14, 2006; Taylor & Francis Inc.: Sydney, Australia, 2006; pp 741−749.
(7) Schmidt, D.; Shah, D.; Giannelis, E. P. *Curr. Opin. Solid State Mater. Sci.* **2002**, *6* (3), 205–212.
(8) Viet, C. X.; Ismail, H.; Rashid, A. A.; Takeichi, T.; Thao, V. H. *Polym.-Plast. Technol. Eng.* **2008**, *47* (11), 1090–1096.
(9) Alexandre, M.; Dubois, P. *Mater. Sci. Eng., R* **2000**, *28* (1−2), 1–63.
(10) Hakim, R. N.; Ismail, H. *J. Reinf. Plast. Compos.* **2009**, *28* (12), 1417–1431.
(11) Arroyo, M.; López-Manchado, M. A.; Herrero, B. *Polymer* **2003**, *44* (8), 2447–2453.
(12) López-Manchado, M. A.; Valentin, J. L.; Herrero, B.; Arroyo, M. *Macromol. Rapid Commun.* **2004**, *25* (14), 1309–1313.
(13) Carretero-González, J.; Valentin, J. L.; Arroyo, M.; Saalwachter, K.; López-Manchado, M. A. *Eur. Polym. J.* **2008**, *44* (11), 3493–3500.
(14) Carretero-González, J.; Retsos, H.; Verdejo, R.; Toki, S.; Hsiao, B. S.; Giannelis, E. P.; López-Manchado, M. A. *Macromolecules* **2008**, *41* (18), 6763–6772.
(15) Pissis, P.; Fragiadakis, D.; Kanapitsas, A.; Delides, K. In *Broadband Dielectric Relaxation Spectroscopy in Polymer Nanocomposites*; 17th European Symposium on Polymer Spectroscopy (ESOPS 17), Seggauberg, Austria, Sept 9−12, 2007; Wiley-VCH Verlag GmbH: Seggauberg, Austria, 2007; pp 12−20.
(16) Fragiadakis, D.; Pissis, P.; Bokobza, L. *Polymer* **2005**, *46* (16), 6001–6008.
(17) Adnan, A.; Sun, C. T.; Mahfuz, H. *Compos. Sci. Technol.* **2007**, *67* (3−4), 348–356.
(18) Mijovic, J.; Lee, H. K.; Kenny, J.; Mays, J. *Macromolecules* **2006**, *39* (6), 2172–2182.
(19) Schönhals, F. K. A. *Broadband Dielectric Spectroscopy*; Springer: Berlin, 2003.
(20) Runt, J. P. *Dielectric Spectroscopy of Polymeric Materials. Fundamentals and Applications*; American Chemical Society: Washington, DC, 1997.
(21) Blythe, A. R. *Electrical Properties of Polymers*; Cambdrige University Press: Oxford, 1979.
(22) Boese, D.; Kremer, F.; Fetters, L. J. *Macromolecules* **1990**, *23* (6), 1826–1830.
(23) Boese, D.; Kremer, F. *Macromolecules* **1990**, *23* (3), 829–835.
(24) Cerveny, S.; Zinck, P.; Terrier, M.; Arrese-Igor, S.; Alegria, A.; Colmenero, J. *Macromolecules* **2008**, *41* (22), 8669–8676.
(25) Page, K. A.; Adachi, K. *Polymer* **2006**, *47* (18), 6406–6413.
(26) Southern Clay Products, Inc., www.scprod.com.
(27) Havriliak, S.; Negami, S. *Polymer* **1967**, *8* (4), 161–210.
(28) Calvet, R. *Clay Clay Miner.* **1975**, *23* (4), 257–265.
(29) Kramarenko, V. Y.; Ezquerra, T. A.; Sics, I.; Balta-Calleja, F. J.; Privalko, V. P. *J. Chem. Phys.* **2000**, *113* (1), 447–452.
(30) Psarras, G. C.; Gatos, K. G.; Karger-Kocsis, J. *J. Appl. Polym. Sci.* **2007**, *106* (2), 1405–1411.
(31) Tsangaris, G. M.; Psarras, G. C.; Kouloumbi, N. *J. Mater. Sci.* **1998**, *33* (8), 2027–2037.
(32) Lee, H. K.; Pejanovic, S.; Mondragon, I.; Mijovic, J. *Polymer* **2007**, *48* (25), 7345–7355.
(33) Hedvig, P. *Dielectric Spectroscopy of Polymers*; Adam Hilger Ltd.: Bristol, 1977.
(34) Kalgaonkar, R. A.; Jog, J. P. *J. Polym. Sci., Part B: Polym. Phys.* **2008**, *46* (23), 2539–2555.
(35) Schonhals, A.; Goering, H.; Schick, C.; Frick, B.; Zorn, R. *Colloid Polym. Sci.* **2004**, *282* (8), 882–891.
(36) Psarras, G. C.; Gatos, K. G.; Karahaliou, P. K.; Georga, S. N.; Krontiras, C. A.; Karger-Kocsis, J. *Express Polym. Lett.* **2007**, *1* (12), 837–845.
(37) Scheidler, P.; Kob, W.; Binder, K. *J. Phys. Chem. B* **2004**, *108* (21), 6673–6686.
(38) Fragiadakis, D.; Pissis, P. *J. Non-Cryst. Solids* **2006**, *353*, 4344–4352.
(39) Petychakis, L.; Floudas, G.; Fleischer, G. *Europhys. Lett.* **1997**, *40* (6), 685–690.
(40) Serghei, A.; Hartmann, L.; Pouret, P.; Leger, L.; Kremer, F. *Colloid Polym. Sci.* **2004**, *282* (8), 946–954.
(41) Fritzsche, J.; Das, A.; Jurk, R.; Stokelhuber, K. W.; Heinrich, G.; Kluppel, M. *Express Polym. Lett.* **2008**, *2* (5), 373–381.
(42) George, S.; Varughese, K. T.; Thomas, S. *J. Appl. Polym. Sci.* **1999**, *73* (2), 255–270.
(43) Abd-El-Messieh, S. L.; Abd-El-Nour, K. N. *J. Appl. Polym. Sci.* **2003**, *88* (7), 1613–1621.